ARTICLE NO. 79-0605R

J80-048

00023
20001

Radiation of an Acoustic Source Near the Trailing Edge of a Wing in Forward Motion

Lu Ting*
New York University, New York, N.Y.

The acoustic sources simulating engine or jet noise located near the trailing edge are considered. During landing or takeoff operations, the flap angle is not small. Solutions for the scattering of the acoustic sources, monopoles, dipoles, or quadrupoles, by the wing with the flap at finite angle are constructed for the case that the acoustic wavelength is much larger than the length of the flap but may be of the same order as the chord. For each given geometry of the flap and the position of the singularities, critical orientations of the dipoles and the quadrupoles are defined along which the noise becomes "suppressed," i.e., the far-field pressure becomes one order smaller.

I. Introduction

ANALYTICAL solutions for the scattering of acoustic sources, monopoles, dipoles, or quadrupoles, by stationary simple bodies were presented in Ref. 1 and compiled in Ref. 2. We shall analyze the scattering of two-dimensional acoustic sources by an airfoil section (Fig. 1). The acoustic sources simulate engine and/or jet noises which are located near the trailing edge. Our problem is complicated because the geometry of the airfoil section with a flap is not simple at all and the motion of the airfoil creates a nonuniform flowfield. We shall simplify our analysis by noting the following facts:

1) The airfoil is thin and at small angle of attack. The order of magnitude of its thickness ratio and the angle of attack will be denoted by δ with

$$\delta \ll 1 \tag{1}$$

2) The length of the flap ℓ is much smaller than that of the chord L, i.e.,

$$\ell / L \ll 1 \tag{2}$$

3) The propagation of subsonic aircraft noise is of prime interest during the landing or takeoff operations; therefore, we have

$$M_\infty \ll 1 \tag{3}$$

where M_∞ is the Mach number of the forward motion.

4) The order of magnitude of the acoustic potential, $\mu\phi(x,y)\exp(-i\omega t)$ is much less than that of the disturbance velocity potential $\delta\phi_0(x,y)$ induced by the airfoil, i.e.,

$$\mu \ll \delta \ll 1 \tag{4}$$

In addition, we shall impose the condition that the acoustic wavelength is much larger than that of the flap, i.e.,

$$\epsilon = k\ell \ll 1 \tag{5}$$

where k is the wavenumber. We do not impose any restriction on kL. The wavelength can be of the same order as the chord.

With the aid of Eqs. (1-5), we will show that the leading term of the acoustic potential obeys the simple convective wave equation. The contributions of the disturbed flowfield around the airfoil will be of the order of δ, except in the small neighborhood of the leading and trailing edges where they will be of the order of M_∞^2 or $M_\infty\epsilon$. We will then utilize condition (5) to define the inner region with the length scale ℓ and the outer region with k^{-1} as the length scale. The solution for the acoustic potential will then be constructed by the method of matched asymptotic expansions with ϵ as the small parameter. This method was suggested by Rayleigh's intuitive arguments[3] and was applied to various acoustic problems in Refs. 4-9.

The two-dimensional velocity potential due to a wing in forward motion, $-U\hat{i}$, and an acoustic source distribution of given frequency ω can be written as

$$\Phi(x,y,t) = Ux + \delta\phi_0(x,y) + \mu\phi(x,y)e^{-i\omega t} \tag{6}$$

The x and y axes are moving with the airfoil and the source. Under condition (4) the governing equation for the acoustic potential linearized with respect to μ can be written as

$$(1-M_\infty^2)\phi_{xx} + \phi_{yy} + 2M_\infty ik\phi_x + k^2\phi = S(x,y) + F(x,y,\phi) \tag{7}$$

where $\omega = kC_\infty$ and $M_\infty = U/C_\infty$. $S(x,y)$ represents the given acoustic source distribution. $F(x,y,\phi)$ is linear in ϕ and represents the influence of the distributed flowfield around the airfoil. It is

$$F(x,y,\phi) = \left[\left(\frac{U+\delta\phi_{0x}}{C}\right)^2 - M_\infty^2\right]\phi_{xx} + \left(\frac{\delta\phi_{0y}}{C}\right)^2\phi_{yy} + 2\frac{(U+\delta\phi_{0x})(\delta\phi_{0y})}{C^2}\phi_{xy} - 2\left[\left(\frac{U+\delta\phi_{0x}}{C}\right)\left(\frac{C_\infty}{C}\right) - M_\infty\right]ik\phi - 2\frac{\delta\phi_{0y}}{C}\left(\frac{C_\infty}{C}\right)ik\phi_y - \left[\left(\frac{C_\infty}{C^2}\right)^2 - 1\right]k^2\phi \tag{8}$$

where

$$C^2 = C_\infty^2 - \frac{\gamma-1}{2}[2U(\delta\phi_{0x}) + (\delta\phi_{0x})^2 + (\delta\phi_{0y})^2]$$

The disturbance potential $\delta\phi_0$ and its derivatives are of the order of δ, except in the small neighborhoods of the length

Presented as Paper 79-0605 at the AIAA 5th Aeroacoustics Conference, Seattle, Wash., March 12-14, 1979; submitted April 30, 1979; revision received Aug. 22, 1979.

Index categories: Aeroacoustics; Noise.

*Professor of Mathematics, Courant Institute of Mathematical Sciences. Member AIAA.

scale ℓ, near the trailing edge and near the leading edge stagnation point. $F(x,y,\phi)$ is of the order of δ times a typical term on the left side of Eq. (7), say ϕ_{xx}, except in the small neighborhoods around the leading and trailing edges where F will be of the order of $M_\infty^2\phi_{xx}$ or $M_\infty\epsilon\phi_{xx}$. From conditions (1), (3), and (5), we conclude that the governing equation for the leading term of the acoustic potential is the convective wave equation

$$(1-M_\infty^2)\phi_{xx}+\phi_{yy}-ikM_\infty\phi_x+k^2\phi=S(x,y) \tag{9}$$

We keep the M_∞^2 terms on the left side of the equation because their influence will be present all the way to the far field. Equation (9) can then be reduced to the simple wave equation by Lorentz transformation.[1]

The boundary conditions in the surface $y=\delta g_\pm(x)$ of the airfoil section and the flap is

$$(U+\delta\phi_{0x}+\mu\phi_x)\delta g'_\pm(x)-(\delta\phi_{0y}+\mu\phi_y)=0 \tag{10}$$

Since the disturbance potential $\delta\phi_0$ fulfills the boundary condition $(U+\delta\phi_{0x})\delta g'_\pm(x)-\delta\phi_{0y}=0$, the boundary condition (10) for the acoustic potential becomes

$$\phi_y-\phi_x\delta g'_\pm(x)=0 \tag{11}$$

Equations (9) and (11) and the radiation condition at the far field define ϕ. Equation (11) can be linearized to

$$\phi_y(x,y=0)=0 \tag{12}$$

for $-kL<kx<0$, where $\delta g'_\pm$ is of the order of δ. Near the leading edge and the flap, $\delta g'$ can be finite and we have to impose the nonlinear boundary condition, Eq. (11).

We will now make use of Eq. (5). With k^{-1} as length scale, the airfoil section in the outer region reduces to the strip $-kL\le\tilde{x}\le 0$, $\tilde{y}=0$ where $\tilde{x}=kx$ and $\tilde{y}=ky$ (see Fig. 2). With ℓ as the length scale, the inner region contains the flap, the source distribution, and the airfoil section near its junction with the flap (see Fig. 3). In the large scale k^{-1}, the inner region shrinks to the trailing edge of the strip in the $\tilde{x}-\tilde{y}$ plane and is represented by equivalent singularities at the trailing edge. The outer solution, $\tilde{\phi}(\tilde{x},\tilde{y})$ and hence the far-field solution can be determined when the equivalent singularities at the trailing of the strip are known. Of course these singularities can be defined only by matching with the inner solution. In the inner region the long wave theory applies. Although the boundary condition cannot be linearized, the solution can be constructed by mapping the inner region in the complex z plane to the right-half ζ plane, where $z=(x+iy)/\ell$ and the solution in the ζ plane can be constructed readily by the method of images.

In the inner region, the airfoil section near the trailing edge is open to infinity, as shown in Fig. 3. There one cannot impose a circulation around it; therefore, one cannot impose a Kutta condition. For example, in a potential flow around a wedge, one cannot impose the Kutta condition. In contrast to our assumption that the acoustic wavelength is only much longer than the flap but can be of the same order as the chord L, Amiet and Sears[4] consider the case that the acoustic wavelength is much larger than the chord length L, i.e., $kL\ll 1$. Therefore, their airfoil section is imbedded in the inner region and the potential flow admits a circulation around the airfoil which is defined by imposing the Kutta condition.

In Sec. II, we specify the class of the mapping functions which will map the inner region in the z plane for a general flap shape to the right-half ζ plane. For each type of acoustic source, a monopole, dipole, or quadrupole, the corresponding singularities in the right-half ζ plane are identified and the solution is constructed by the method of images. The inner solution in the z plane is then obtained from the mapping function. The equivalent singularities at the trailing edge for the outer region are determined by matching with the inner solution for large z and the outer solution is then constructed. For a given location of the dipole or quadrupole relative to the flap, the solution defines a critical orientation so that the far-field intensity will be reduced by an order of magnitude. Numerical examples for a simple flap shape is presented in Sec. III.

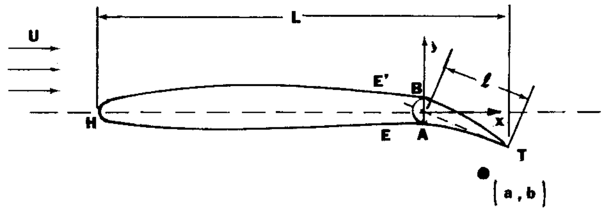

Fig. 1 Acoustic source near the trailing edge.

Fig. 2 Outer region.

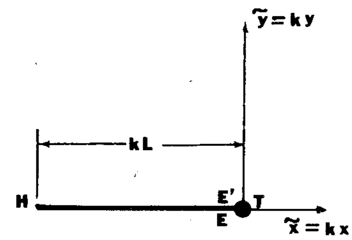

Fig. 3 Inner region.

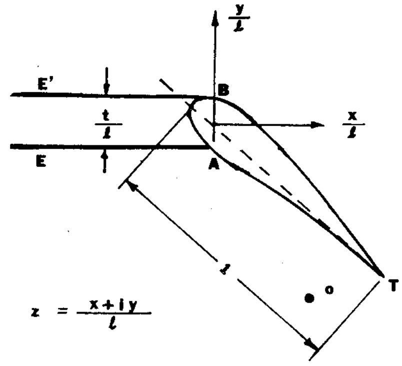

II. Acoustic Sources Near the Trailing Edge

We shall construct the inner solution for a wing with its flap down at an angle $\lambda\pi$. Let ℓ denote the reference length of the flap, the small parameter for our problem will be $k\ell$, i.e.,

$$\epsilon=k\ell\ll 1 \tag{13}$$

With ℓ as the reference length scale, the complex z plane, with $z=(x+iy)/\ell$, shows the inner region of our problem (Fig. 3). The upper and lower surfaces of the basic airfoil section become lines parallel to the negative x axis. We shall map the domain outside the airfoil and its flap into the right-half ζ plane by the conformal transformation

$$\zeta=F(z) \quad \text{or} \quad z=G(\zeta) \tag{14}$$

The construction of the mapping function for a given flap geometry is a standard mathematical problem. In general, the function $F(z)$ should behave as $\sqrt{z}$ for large z because the locally enlarged shape of the basic airfoil section becomes a strip parallel to the negative x/ℓ axis. We expect the function $dz/d\zeta$ to be a descending power series in ζ for large ζ with 2ζ as the leading term,

$$\frac{dz}{d\zeta}=G'(\zeta)=2\zeta+id_1+\frac{d_2}{\zeta}+\frac{id_3}{\zeta^2}+\ldots \tag{15}$$

where the d_j's are real numbers because $dz/d\zeta$ should be imaginary along the imaginary ζ axis. From Eq. (15), it follows

$$z=G(\zeta)=\zeta^2+id_1\zeta+d_0+d_2\ln\zeta+0(1/\zeta) \quad (16)$$

and the inverse transformation for large z is

$$\zeta=F(z)=\sqrt{z}+ic_0-\frac{d_2}{2\sqrt{z}}\ln z+\frac{c_2}{\sqrt{z}}+\ldots \quad (17)$$

The coefficients, c_j's, are real and are related to the d_j's, i.e.,

$$c_0=-d_1/2, \quad c_2=-(d_0+d_1^2/4)/2$$

From Eq. (16), we note that the imaginary part of z is $\pm d_2\pi/2$ when $\zeta=\pm i\eta$ for large positive real η. Therefore, the thickness of the airfoil at its junction near the flap is $d_2\pi\ell$. It should be of the order $(\pi\tau)\ell$, where $\pi\tau$ is the trailing-edge angle. Since $\tau\pi$ is of the order of the thickness ratio of the airfoil δ, we have

$$d_2=O(\tau)=O(\delta/\pi)\ll 1 \quad (18)$$

At the onset, we have neglected terms of the order δ in the acoustic equations, the contributions of terms involving d_2 can be ignored.

For a singularity located at $z_0=(a+ib)/\ell$, its image in the ζ plane is:

$$\zeta_0=|\zeta_0|e^{i\nu_0}=F(z_0) \quad (19)$$

In the following three subsections we will construct the solutions for monopoles, dipoles, and quadrupoles, respectively.

A. Solution for a Monopole

When the singularity is a monopole, its acoustic potential in free space can be written as

$$\phi^{(i)}=(-im/4)H_0^{(1)}(k\rho) \quad (20)$$

where $H_\nu^{(1)}$ is the Hankel function of the first kind of order ν, $\rho=[(x-a)^2+(y-b)^2]^{1/2}$ and m is the strength of the monopole. For small $k\rho$, we have

$$\phi^{(i)}=\frac{m}{2\pi}\left[\ln\left(\frac{1}{2}Bk\rho\right)-\frac{i\pi}{2}+0(\rho)\right]$$

$$=\frac{m}{2\pi}\left[\ln|z-z_0|+\ln\left(\frac{1}{2}B\epsilon\right)-\frac{i\pi}{2}+0(\rho)\right]$$

$$=\frac{m}{2\pi}\left[\ln|G(\zeta)-G(\zeta_0)|+\ln\left(\frac{1}{2}B\epsilon\right)-\frac{i\pi}{2}+0(\zeta-\zeta_0)\right] \quad (21)$$

where B is the Euler constant. To identify the singularity in the ζ plane at ζ_0, we note the Taylor series for $G(\zeta)$,

$$z-z_0=G(\zeta)-G(\zeta_0)=(\zeta-\zeta_0)G'(\zeta_0)\{1$$

$$+\tfrac{1}{2}[G''(\zeta_0)/G'(\zeta_0)](\zeta-\zeta_0)+0(\zeta-\zeta_0)^2\} \quad (22)$$

and obtain from Eq. (21)

$$\phi^{(i)}=\frac{m}{2\pi}\left\{\ln|\zeta-\zeta_0|+\ln\left(\frac{1}{2}B\epsilon g_1\right)-\frac{i\pi}{2}+i\nu_1+0|\zeta-\zeta_0|\right\} \quad (23)$$

with $|G'(\zeta_0)|=g_1$ and $\nu_1=\arg G'(\zeta_0)$. Equation (22) shows that in the near field the singularity becomes a potential source of the same strength located at $\zeta=\zeta_0$. In the ζ plane, the imaginary axis represents the rigid surface of the plate. The solution for the complex potential function $\chi(z)$ with only one singular point at $\zeta=\zeta_0$ in the right-half plane is obtained by the addition of the image at $\zeta=-\zeta^*$ in the left-hand plane (see Fig. 4). The result is:

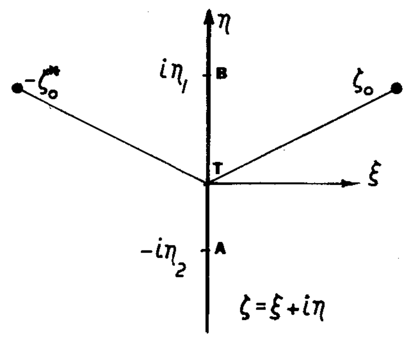

Fig. 4 ζ plane, the singular point and its image.

$$\chi(\zeta,a,b)=\frac{m}{2\pi}\{\ln(\zeta-\zeta_0)+\ln(\zeta+\zeta_0^*)\} \quad (24)$$

where (*) means "the conjugate of." For large ζ, we have

$$\chi=\frac{m}{2\pi}\left\{\ln\zeta^2-\frac{2i}{\zeta}(Im\zeta_0)+0\left(\frac{1}{\zeta^2}\right)\right\} \quad (25)$$

Using the mapping function for large ζ, we obtain the expression for x at large z,

$$\chi=\frac{m}{2\pi}\left\{\ln z-\frac{2i}{\sqrt{z}}(Im\zeta_0-c_0)+0\left(\frac{1}{z}\right)\right\} \quad (26)$$

The first term represents a point source and the second term represents a flow around the edge of the plate. The acoustic potential of the inner region for large (r/ℓ) is

$$\bar{\phi}=Re\chi+\frac{m}{2\pi}K_1=\frac{m}{2\pi}\left\{\ln\frac{r}{\ell}-\left(\frac{\ell}{r}\right)^{1/2}(Im\zeta_0-c_0)\sin\frac{\theta}{2}+0\left(\frac{\ell}{r}\right)+K_1\right\} \quad (27)$$

where $r\exp(i\theta)=x+iy$ and K_1 is a constant to be defined. For large r but small kr, which is $\bar{r}$, Eq. (27) becomes

$$\bar{\phi}=\frac{m}{2\pi}\left\{\ln\bar{r}-\ln\epsilon+2\left(\frac{\epsilon}{\bar{r}}\right)^{1/2}(Im\zeta_0-c_0)\sin\frac{\theta}{2}+0(\epsilon)+K_1\right\} \quad (28)$$

This equation defines the singular behavior of the outer solution near the trailing edge. The outer solution fulfilling this matching condition and the radiation condition is:

$$\tilde{\phi}=-\frac{im}{4}\left\{H_0^{(1)}(\bar{r})+4\left(\frac{2\epsilon}{\pi}\right)^{1/2}(|\zeta_0|\sin\nu_0-c_0)\cdot\left[H_{1/2}^{(1)}(\bar{r})\sin\frac{\theta}{2}+\phi^{(s)}\right]+0(\epsilon)\right\} \quad (29)$$

As shown in Fig. 2, the airfoil reduces to a strip, $-kL<kx<0$ and $ky=\pm 0$. The first term $H_0^{(1)}(\bar{r})$ is a monopole at the trailing of the strip. It is symmetric with respect to the x axis; therefore, there is no scattering solution for finite kL. The second term represents the asymmetric effect of the location of the monopole and that of the geometry of the flap, $|\zeta_0|\sin\nu_0-c_0$. The asymmetric solution $H_{1/2}^{(1)}(\bar{r})\sin\theta/2$ represents a singularity at the trailing edge and fulfills the boundary condition on the strip, but it creates a discontinuity ahead of the leading ege $\tilde{x}<-kL$ by the amount $2H_{1/2}^{(1)}(|\tilde{x}|)$ as $ky\to\pm 0$, $\theta\to\pm\pi$. The sheet of discontinuity shall be removed by the scattering solution $\phi^{(s)}(\tilde{x},\tilde{y})$, which can be constructed by the standard procedures[2] for the solutions of the reduced wave equation exterior to the rigid strip, $-kL<\tilde{x}<0$, $y=0^{\pm}$. It is a canonical problem in the sense that it is independent of the geometry of the airfoil section. $\phi^{(s)}$ shall be split into two parts, $\phi_1^{(s)}$ and $\phi_2^{(s)}$. Each one of them fulfills the reduced wave equation. $\phi_1^{(s)}$ is the solution of the half-space problem; $\tilde{y}>0$ with the Dirichlet boundary condition on $\tilde{y}=0^+$,

$$\phi_1^{(s)}=-H_{1/2}^{(1)}(|\tilde{x}|) \quad \text{for} \quad \tilde{x}<-kL$$

and

$$\phi_1^{(s)}=0 \qquad \text{for} \quad x>-kL$$

The solution $\phi_1^{(s)}$ is then extended by $\tilde{y}<0$ as an odd function in $\tilde{y}$, i.e.,

$$\phi_1^{(s)}(\tilde{x},\tilde{y})=-\phi_1^{(s)}(\tilde{x},-\tilde{y}) \qquad \text{for } \tilde{y}<0$$

Thus, the solution $\phi_1^{(s)}(\tilde{x},\tilde{y})$ removes the sheet of discontinuity on $\tilde{y}=0$, $\tilde{x}<-kL$ due to $H_{1/2}^{(1)}(\tilde{r})\sin(\theta/2)$. On the other hand, $\phi_1^{(s)}$ creates nonzero normal velocity on the rigid strip, which shall be removed by the second part $\phi_2^{(s)}$. The boundary condition for $\phi_2^{(s)}$ is:

$$[\phi_2^{(s)}]_{\tilde{y}}=-[\phi_1^{(s)}]_{\tilde{y}} \quad \text{for} \quad \tilde{y}=0^{\pm}, \quad -kL<\tilde{x}<0$$

The solution to this Neumann problem can be constructed by the method of separation of variables in terms of the elliptical cylindrical coordinates.[2]

The constant K_1 in Eq. (28) is defined by comparing with Eq. (29). We have

$$K_1=\ln(Bg_1/2) \tag{30}$$

B. Solution for a Dipole

A dipole in free space can, in general, be expressed as derivatives of a monopole

$$\phi^{(i)}=\left(D_1\frac{\partial}{\partial a}+D_2\frac{\partial}{\partial b}\right)\left[-\frac{i}{4}H_0^{(1)}(k\rho)\right] \tag{31}$$

where D_1 and D_2 denote the two components of the dipole. This equation yields

$$\phi^{(i)}=-\frac{ik}{4\rho}[D_1(x-a)+D_2(y-b)]H_1^{(1)}(k\rho) \tag{32}$$

For small $k\rho$, we have

$$\phi^{(i)}=-\frac{1}{2\pi}\left\{D_1\frac{x-a}{\rho^2}+D_2\frac{y-b}{\rho^2}+0(k\rho\ln k\rho)\right\}$$

$$=Re\left\{\frac{D}{\ell}e^{i\alpha}\left(\frac{-1}{2\pi}\right)\frac{1}{z-z_0}\right\}+0(k\rho\ln k\rho)\Big\} \tag{33}$$

It represents a doublet at z_0 with strength D and an inclination α with $D\exp(i\alpha)=D_1+iD_2$.

From Eq. (22) we obtain the singular behavior of the complex potential χ in the right-half ζ plane,

$$\chi\sim\frac{-D}{2\pi\ell}e^{i\alpha}\left[\frac{1}{G'(\zeta_0)}\right]\frac{1}{\zeta-\zeta_0} \tag{34}$$

It represents a doublet with strength modified by the factor $[G'(\zeta_0)]^{-1}$. With the imaginary axis as the line of symmetry, the complex potential is:

$$\chi=\frac{-D}{2\pi\ell g_1}\left[\frac{e^{i(\alpha-\nu_1)}}{\zeta-\zeta_0}-\frac{e^{-i(\alpha-\nu_1)}}{\zeta+\zeta_0^*}\right] \tag{35}$$

For large ζ, Eq. (35) yields

$$\chi=-\frac{iD\sin(\alpha-\nu_1)}{\pi\ell g_1}\left(\frac{1}{\zeta}\right)-\frac{D|\zeta_0|\cos(\alpha-\nu_1+\nu_0)}{\pi\ell g_1}\left(\frac{1}{\zeta^2}\right)$$

$$+0\left(\frac{1}{\zeta^3}\right) \tag{36}$$

Using the mapping function for large z, we obtain the acoustic potential of the inner region for large (r/ℓ)

$$\bar{\phi}=Re\chi=-\frac{D\sin(\alpha-\nu_1)}{\pi\ell g_1}\left(\frac{\ell}{r}\right)^{1/2}\sin\frac{\theta}{2}$$

$$-\frac{D}{\pi\ell g_1}[|\zeta_0|\cos(\alpha-\nu_1+\nu_0)+c_0\sin(\alpha-\nu_1)]\left(\frac{\ell}{r}\right)\cos\theta$$

$$+K_2+0(\epsilon^{1/2}) \tag{37}$$

K_2 is a constant to be defined by matching with the outer solution. Replacing r by $\tilde{r}/k$, we obtain from the last equation the behavior of the outer solution, $\tilde{\phi}$, for small $\tilde{r}$. The corresponding outer solution is:

$$\tilde{\phi}=-\frac{ikD}{2g_1}\left\{\left(\frac{2}{\pi\epsilon}\right)^{1/2}\sin(\alpha-\nu_1)\left[H_{1/2}^{(1)}(\tilde{r})\sin\frac{\theta}{2}+\phi^{(s)}\right]\right.$$

$$+[|\zeta_0|\cos(\alpha-\nu_1+\nu_0)+c_0\sin(\alpha-\nu_1)]H_1^{(1)}(\tilde{r})$$

$$\left.\times\cos\theta+0(\epsilon^{1/2})\right\} \tag{38}$$

$\phi^{(s)}$ is the same scattering solution introduced in Eq. (29) to remove the sheet of discontinuity ahead of the leading edge of the strip due to the asymmetric solution $H_{1/2}^{(1)}(\tilde{r})\sin\theta/2$. The second term, $H_1^{(1)}(\tilde{r})\cos\theta$, is symmetric with respect to the $\tilde{x}$ axis and therefore fulfills the boundary condition for the strip.

The second term represents a dipole located at the origin and oriented along the x axis. The first term represents the asymmetric effects due to the geometry of the flap, the orientation, and the location of the dipole. The asymmetric term is of the order of $\epsilon^{-1/2}$ as compared to the symmetric dipole term. It should be noted that in the analysis the amplitudes D_1 and D_2 of the dipole are kept the same as those in the free space. The energy flux required to sustain the same amplitudes will not be the same as that in the free space. If we keep the energy flux of the dipole the same as that in the free space, the asymmetric term in Eq. (38) will be of the order ϵ^0, while the symmetric dipole term will be of the order $\epsilon^{1/2}$.

The leading term in Eq. (38) vanishes when α equals ν_1. This means that for a given dipole location z_0, and the flap geometry $G(\zeta)$, there is a critical orientation of the dipole with

$$\arg(D_1+iD_2)=\alpha_c=\arg G'(\zeta_0) \tag{39}$$

at which the outer solution is reduced by an order of $\sqrt{\epsilon}$.

We can also obtain the inner solution for the doublet, Eq. (35), by applying the differential operator $D_1\,\partial/\partial a+D_2\partial/\partial b$ to the inner solution for the monopole, Eq. (27), with $m=1$. We cannot employ the same procedure to obtain the outer solution, Eq. (38), because in the outer solution for the monopole, Eq. (29), it is placed at the origin of the $\tilde{x}-\tilde{y}$ plane and the dependence on the location (a,b) is lost as both ka and kb approach zero.

C. Solution of a Quadrupole

A quadrupole in free space can, in general, be expressed as

$$\phi^{(i)} = \left[Q_{11}\frac{\partial^2}{\partial a^2} + (Q_{12}+Q_{21})\frac{\partial^2}{\partial a\partial b} + Q_{22}\frac{\partial^2}{\partial b^2}\right] \cdot \left[\frac{-i}{4}H_0^{(1)}(k\rho)\right] \tag{40}$$

where the constant matrix $[Q_{ij}]$ defines the strength of the quadrupole. Since $H_0^{(1)}(k\rho)$ obeys the reduced wave equation with respect to a,b, we have

$$\phi^{(i)} = -\frac{ik^2}{8}\{(Q_{11}-Q_{22})H_2^{(1)}(k\rho)\cos 2\psi - (Q_{11}+Q_{22})H_0^{(1)}(k\rho) + (Q_{12}+Q_{21})H_2^{(1)}(k\rho)\sin 2\psi\} \tag{41}$$

where $\psi = \tan^{-1}[(y-b)/(x-a)]$. For small $k\rho$, we have

$$\phi^{(i)} \sim -\frac{\cos 2\psi}{2\pi\rho^2}(Q_{11}-Q_{22}) - \frac{\sin 2\psi}{2\pi\rho^2}(Q_{12}+Q_{21}) + \frac{k^2}{2\pi}(Q_{11}+Q_{22})\ln(\rho k) \tag{42}$$

The first two terms represent a potential quadrupole, while the last term represents a potential source. Consequently, the inner solution will be split into two terms, $\bar{\phi}_1$ and $\bar{\phi}_2$, representing, respectively, the potential solutions induced by the quadrupole and the source in the presence of a semi-infinite plate. We write

$$\bar{\phi} = \bar{\phi}_1 + \bar{\phi}_2$$

The solution $\bar{\phi}_2$ and the corresponding outer solution are given by Eqs. (23) and (25) when the strength m is identified as $k^2(Q_{11}+Q_{22})$.

We can now define the strength of the quadrupole in Eq. (42) by a vector

$$(Q_{11}-Q_{22}) + (Q_{12}+Q_{21})i = Qe^{i\alpha} \tag{43}$$

The first two terms in Eq. (42) be rewritten as the real part of $\chi_1^{(i)}(z)$ with

$$\begin{aligned}\chi_1^{(i)}(z) &= -\frac{Q}{2\pi\ell^2}e^{i\alpha}(z-z_0)^{-2} = -\frac{Q}{2\pi\ell^2}e^{i\alpha}[G(\zeta)-G(\zeta_0)]^{-2} \\ &= -\frac{Q}{2\pi\ell^2}e^{i\alpha}[(\zeta-\zeta_0)G'(\zeta_0)]^{-2} \cdot \{1+\tfrac{1}{2}[G''(\zeta_0)/G'(\zeta_0)](\zeta-\zeta_0)+\ldots\}^{-2} \\ &= -\frac{Q}{2\pi\ell^2 g_1^2}e^{i(\alpha-2\nu_1)}\frac{1}{(\zeta-\zeta_0)^2} + \frac{Qg_2}{2\pi\ell^2 g_1^3}e^{i(\alpha-3\nu_1+\nu_0)}\cdot\frac{1}{\zeta-\zeta_0} + O(1)\end{aligned} \tag{44}$$

where $g_2 = |G''(\zeta_0)|$ and $\nu_2 = \arg G''(\zeta_0)$. Those two terms in Eq. (44) represent a quadrupole and a dipole at $\zeta=\zeta_0$. They define the singularities of $\bar{\phi}_1$ in the right-half ζ plane. The complex potential χ_1 is obtained by the addition of the images at $\zeta = -\zeta_0^*$. The result is:

$$\chi_1 = -\frac{Q}{2\pi\ell^2 g_1^2}\left\{\frac{1}{(\zeta-\zeta_0)^2}e^{i(\alpha-2\nu_1)} + \frac{1}{(\zeta+\zeta_0^*)^2}e^{-i(\alpha-2\nu_1)}\right\} + \frac{Qg_2}{2\pi\ell^2 g_1^3}\left\{\frac{1}{\zeta-\zeta_0}e^{i(\alpha-3\nu_1+\nu_2)} - \frac{1}{\zeta+\zeta_0^*}e^{-i(\alpha-3\nu_1+\nu_2)}\right\} \tag{45}$$

For large ζ, we have

$$\chi_1 = \frac{Q}{\pi g_1^2\ell^2}\left\{i\frac{g_2}{g_1}\frac{\sin(\alpha-3\nu_1+\nu_2)}{\zeta} + \frac{E_2}{\zeta^2} + \frac{iE_3}{\zeta^3} + \frac{E_4}{\zeta^4} + O\left(\frac{1}{\zeta^5}\right)\right\} \tag{46}$$

where

$$E_2 = [\,|\zeta_0|g_2/g_1]\cos(\alpha-3\nu_1+\nu_2+\nu_0) - \cos(\alpha-2\nu_1)$$

$$E_3 = \{[\,|\zeta_0|g_2/g_1]\sin(\alpha-3\nu_1+\nu_2+2\nu_0) - 2\sin(\alpha-2\nu_1+\nu_0)\}\,|\zeta_0|$$

$$E_4 = \{[\,|\zeta_0|g_2/g_1]\cos(\alpha-3\nu_1+\nu_2+3\nu_0) - 3\cos(\alpha-2\nu_1+2\nu_0)\}\,|\zeta_0|^2$$

Using the mapping function for large z, we have the expression for χ_1 at large z,

$$\chi_1 = \frac{Q}{\pi g_1^2\ell^2}\left\{i\frac{g_2}{g_1}\frac{\sin(\alpha-3\nu_1+\nu_2)}{\sqrt{z}} + \frac{A_2}{z} + \frac{iA_2}{z^{3/2}} + \frac{A_4}{z^2} + O(z^{-5/2})\right\} \tag{47}$$

where

$$A_2 = E_2 + c_0E_1$$

$$A_3 = E_3 - (c_2+c_0^2)E_1 - 2c_0E_2$$

$$A_4 = E_4 - (c_0^3+2c_2c_0-c_3)E_1 - [3c_0^2+2c_2]E_2 + 3c_0E_3$$

with $E_1 = (g_2/g_1)\sin(\alpha-3\nu_1+\nu_2)$.

By repeating the matching procedure, we obtain the outer solution,

$$\begin{aligned}\tilde{\phi}(\tilde{r},\theta) = \frac{Qk^2 i}{2g_1^2}\Big\{&\epsilon^{-3/2}\left(\frac{2}{\pi}\right)^{1/2}\frac{g_2}{g_1}\sin(\alpha-3\nu_1+\nu_2) \times [H_{1/2}^{(1)}(\tilde{r})\sin\theta/2 + \phi^{(s)}] + \epsilon^{-1}A_2H_1^{(1)}(\tilde{r})\cos\theta \\ &+ \epsilon^{-1/2}A_3\left(\frac{2}{\pi}\right)^{1/2}[H_{3/2}^{(1)}(\tilde{r})\sin(3\theta/2) + \psi^{(s)}] + \frac{1}{2}A_4H_2^{(1)}(\tilde{r})\cos 2\theta\Big\} - \frac{ik^2}{4}(Q_{11}+Q_{22})H_0^{(1)}(r) + O(\epsilon^{1/2})\end{aligned} \tag{48}$$

The function $\psi^{(s)}$ is the scattering solution which removes the discontinuity created by $H_{3/2}^{(1)}(\tilde{r})\sin(3\theta/2)$ ahead of the leading edge of the strip. $\psi^{(s)}$ can be obtained by the same procedure outlined for $\phi^{(s)}$ in Eq. (38).

Similar to the solution for dipoles, the leading term is the one due to the asymmetry of the flap and the location and orientation of the quadrupole. For the outer solution, it appears as the asymmetric edge effect at the trailing edge of the strip. It is of the order of $\epsilon^{-3/2}$ larger than the fourth term, which is the solution of an equivalent quadrupole at the trailing edge and oriented along the strip. If we maintain the same amplitudes for the quadrupole, then the energy flux required to sustain the quadrupole in the presence of the airfoil will be of the order ϵ^{-3} times that in the free space. If we maintain the same energy flux, then the amplitude of the quadrupole in the presence of the airfoil will be of the order of $\epsilon^{3/2}$ times that in the free space.

The first term in Eq. (48) vanishes when

$$\alpha=\alpha_c=3\nu_1-\nu_2$$

that is,

$$\frac{Q_{12}+Q_{21}}{Q_{11}-Q_{22}}=\tan\alpha_c=\tan(3\nu_1-\nu_2) \tag{49}$$

We recall that $\nu_1=\arg G'(\zeta_0)$ and $\nu_2=\arg G''(\zeta_0)$; therefore, at each location, z_0 or ζ_0, there is a critical orientation α_c, such that the outer solution and the far-field pressure will be reduced by an order of $\sqrt{\epsilon}$.

The second term in Eq. (48) vanishes also when $E_2=0$, which yields the condition

$$|\zeta_0|\cos\nu_0=(g_1/g_2)\cos(\nu_1-\nu_2)$$

that is,

$$Re[\zeta_0-G'(\zeta_0)/G''(\zeta_0)]=0 \tag{50}$$

This defines a curve in the ζ plane. When the quadrupole is located on the image of the curve, Eq. (50), in the z plane and is oriented at the critical angle, Eq. (49), the outer solution and the far-field pressure will be reduced by the order ϵ.

For the special mapping function $z=\zeta^2$, the airfoil and the flap became a semi-infinite plate. We have $G'(\zeta_0)=2\zeta_0$, $G''=2$, $\nu_1=\nu_0$, $\nu_2=0$, $g_1=2|\zeta_0|$ and $g_2=2$. The solutions for the monopole, dipole, and the quadrupole are in agreement with the corresponding expressions in Ref. 10, in which the solutions for the semi-infinite plate were constructed without making use of the Taylor series expansion of $G(\zeta)$ near ζ_0.

III. An Example

The preceding analyses were carried out for a class of mapping functions defined by Eq. (15). We will demonstrate how to determine these coefficients d_j in Eq. (15) for a given flap geometry as shown in Fig. 5. The upper and lower surfaces of the flap, AT and TB, are planes inclined at angles $-\pi\lambda$ and $-\pi(\lambda+\tau)$, respectively, to the x axis. The trailing edge angle is $\tau\pi$. The length of AT is designed as the length scale ℓ. The lower and upper surfaces, EA and EB, of the airfoil near the junction with the flap are represented by the lines $y=-t/2$ and $y=t/2$, respectively. The point A is located at $(0,-t/2)$. The length of the upper surface of the flap, TB, is related to the airfoil thickness t by the relationship

$$\frac{\ell'}{\ell}=1+\frac{(t/\ell)-2\sin(\tau\pi/2)\cos[(\lambda+\tau/2)\pi]}{\sin[(\lambda+\tau)\pi]} \tag{51}$$

It is clear that ℓ' differs from ℓ slightly since t/ℓ and $\tau\pi$ are small. The mapping function from the ζ plane to the right-half plane is given by the Schwartz-Christoffel transformation

$$G'(\zeta)=\frac{dz}{d\zeta}=\frac{2\zeta^{1-\tau}(\zeta-i\eta_1)^{\lambda+\tau}}{(\zeta+i\eta_2)^{\lambda}} \tag{52}$$

Points A, T, and B in the ζ plane are located at the $\zeta=-i\eta_2$, $\zeta=0$, and $\zeta=i\eta_1$ respectively, where η_1 and η_2 are positive real numbers. For large ζ, we have

$$\frac{dz}{d\zeta}=2\zeta\left(1-\frac{i\eta_1}{\zeta}\right)^{\lambda+\tau}\left(1+\frac{i\eta_2}{\zeta}\right)^{-\lambda}$$

$$=2\zeta-2i[(\lambda+\tau)\eta_1+\lambda\eta_2]-(1/\zeta)\{(\lambda+\tau)(\lambda+\tau-1)\eta_1^2$$

$$+2(\lambda+\tau)\lambda\eta_1\eta_2+\lambda(\lambda+1)\eta_2^2\}+0(1/\zeta^2) \tag{53}$$

By equating coefficients of ζ^j, we define the coefficients d_j in Eq. (15) in terms of η_1 and η_2. These two constants are defined by the geometry of the flap. They are:

$$t/\ell=\pi d_2=\pi\{(\lambda+\tau)p^2-\lambda-[(\lambda+\tau)p+\lambda]^2\}\eta_2^2 \tag{54}$$

and

$$\frac{|TA|}{\ell}=1=2\int_{-\eta_2}^{0}d\eta\frac{|\eta|^{1-\tau}|\eta-\eta_1|^{\lambda+\tau}}{(\eta+\eta_2)^{\lambda}}$$

$$=2\eta_2^2\int_{-1}^{0}d\eta\frac{|\eta|^{1-\tau}|\eta-p|^{\lambda+\tau}}{(\eta+1)^{\lambda}} \tag{55}$$

where $p=\eta_1/\eta_2$. We can eliminate η_2 from these two equations and establish a relationship between t/ℓ and p. Since t/ℓ is positive, we see that p should be nearly equal to but greater than p_c with

$$p_c=\frac{\lambda(\lambda+\tau)+[(\lambda+\tau)(1-\tau)\lambda]^{1/2}}{(1-\lambda-\tau)(\lambda+\tau)} \tag{56}$$

Figure 6 shows t/ℓ and η_2 as functions of p for a 30 deg flap angle and a 6 deg trailing-edge angle, i.e., $\lambda=1/6$ and $\tau=1/30$.

After the determination of η_1 and η_2 in terms of t/ℓ, λ, and τ, the mapping function is defined by the equation

$$z=G(\zeta)=-\frac{it}{\ell}+e^{-i\pi\lambda}+\int_0^{\zeta}d\zeta G'(\zeta) \tag{57}$$

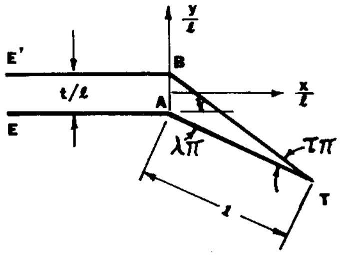

Fig. 5 Simple flap.

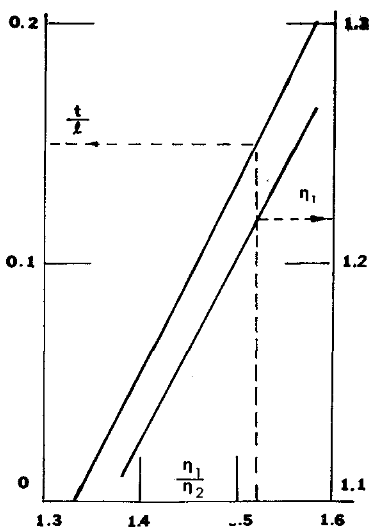

Fig. 6 Relationship between t/ℓ, η_1 and η_2 for $\lambda=1/6$ and $\tau=1/30$.

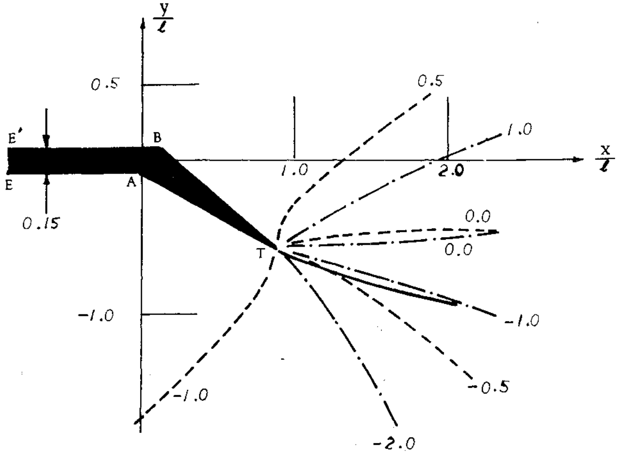

Fig. 7 Lines of constant critical angle α_c for dipole and those for quadrupole.

The constant d_0 in Eq. (16) is defined by the equation

$$d_0 = \lim_{\zeta \to \infty} \{ z - (\zeta^2 + i d_1 \zeta + d_2 \ln \zeta) \}$$

$$= \cos\lambda\pi - \frac{\ell'}{\ell} \cos(\lambda+\tau)\pi + 2\eta_1^2 + d_1\eta_1 - d_2 \ln \eta_1$$

$$- \int_{\eta_1}^{\infty} d\eta \left\{ \frac{2|\eta|^{1-\tau} |\eta - \eta_1|^{\lambda+\tau}}{(\eta+\eta_2)^{\lambda}} - 2\eta - d_1 + \frac{d_2}{\eta} \right\} \tag{58}$$

With the constants η_1 and η_2 defined by Eqs. (54) and (55), we can plot the lines of constant critical angles for dipoles, Eq. (39), and for quadrupoles, Eq. (49). Those lines are shown in Fig. 7 for the case of $t/\ell = 0.15$, $\lambda = 1/6$, and $\tau = 1/30$. The curve defined by Eq. (50) is shown as the solid line in Fig. 7. For a quadrupole located on the solid line and oriented along the critical angle, Eq. (49), the leading two terms in the outer solution, Eq. (48) vanish, i.e., the far-field pressure is reduced by an order of ϵ.

IV. Conclusion

We have shown that when the acoustic wavelength is much larger than the length of the flap, the solution for the radiation of a point source near the flap can be reduced to two relatively simple ones which can be constructed by standard methods. They are: 1) the inner solution which requires the construction of a mapping function that maps the flowfield near the flap to a half plane, and 2) the outer solution for the scattering by a flat plate with singularities specified at the trailing edge with the plate in forward motion at a uniform velocity parallel to the plate.

Acknowledgment

This research is supported by NASA Grant NSG-1469.

References

[1] Morse, P. M. and Ingard, K. U., *Theoretical Acoustics*, McGraw-Hill Book Co., New York, 1968, pp. 400-463 and 698-760.

[2] Bowman, J. J., Senior, T.B.A., and Uslenghi, P.L.E., *Electromagnetic and Acoustic Scattering by Simple Shapes*, John Wiley, New York, 1969, pp. 181-239.

[3] Rayleigh, Lord, *Theory of Sound*, Dover Publications, New York, 1945, re-issue, pp. 196-201 and 487-491.

[4] Amiet, R. and Sears, W. R., "The Aerodynamic Noise of Small Perturbation Subsonic Flow," *Journal of Fluid Mechanics*, Vol. 44, Nov. 1970, pp. 227-235.

[5] Lesser, M. B. and Lewis, J. A., "Applications of Matched Asymptotic Expansion Methods to Acoustics I," *Journal of the Acoustical Society of America*, Vol. 51, May 1972, pp. 1664-1669.

[6] Lesser, M. B. and Lewis, J. A., "Applications of Matched Asymptotic Methods to Acoustics II," *Journal of the Acoustical Society of America*, Vol. 52, Nov. 1972, pp. 1406-1410.

[7] Ting, L. and Keller, J. B., "Radiation from the Open End of a Cylindrical or Conical Pipe and Scattering From the End of a Rod or a Slab," *Journal of the Acoustical Society of America*, Vol. 61, June 1977, pp. 1433-1444.

[8] Ting, L., "Sound Propagation Through a Subsonic Jet Due to a Source Near the Duct Exit," *Journal of Sound and Vibration*, Vol. 57, April 1978, pp. 523-534.

[9] Callegari, A. J. and Myers, M. K., "On the Singular Behavior of Linear Acoustic Theory in Near-Sonic Duct Flows," *Journal of Sound and Vibration*, Vol. 51, April 1977, pp. 517-531.

[10] Ting, L., "Radiation of an Acoustic Source Near the Trailing Edge of a Wing in Forward Motion," AIAA Paper 79-0605, March 1979.